Fermilab-Pub-08/271-E

Search for scalar leptoquarks and T-odd quarks in the acoplanar jet topology using 2.5 fb^{-1} of $p\bar{p}$ collision data at $\sqrt{s}$ =1.96 TeV

V.M. Abazov[36], B. Abbott[75], M. Abolins[65], B.S. Acharya[29], M. Adams[51], T. Adams[49], E. Aguilo[6], M. Ahsan[59], G.D. Alexeev[36], G. Alkhazov[40], A. Alton[64,a], G. Alverson[63], G.A. Alves[2], M. Anastasoaie[35], L.S. Ancu[35], T. Andeen[53], B. Andrieu[17], M.S. Anzelc[53], M. Aoki[50], Y. Arnoud[14], M. Arov[60], M. Arthaud[18], A. Askew[49], B. Åsman[41], A.C.S. Assis Jesus[3], O. Atramentov[49], C. Avila[8], F. Badaud[13], L. Bagby[50], B. Baldin[50], D.V. Bandurin[59], P. Banerjee[29], S. Banerjee[29], E. Barberis[63], A.-F. Barfuss[15], P. Bargassa[80], P. Baringer[58], J. Barreto[2], J.F. Bartlett[50], U. Bassler[18], D. Bauer[43], S. Beale[6], A. Bean[58], M. Begalli[3], M. Begel[73], C. Belanger-Champagne[41], L. Bellantoni[50], A. Bellavance[50], J.A. Benitez[65], S.B. Beri[27], G. Bernardi[17], R. Bernhard[23], I. Bertram[42], M. Besançon[18], R. Beuselinck[43], V.A. Bezzubov[39], P.C. Bhat[50], V. Bhatnagar[27], C. Biscarat[20], G. Blazey[52], F. Blekman[43], S. Blessing[49], K. Bloom[67], A. Boehnlein[50], D. Boline[62], T.A. Bolton[59], E.E. Boos[38], G. Borissov[42], T. Bose[77], A. Brandt[78], R. Brock[65], G. Brooijmans[70], A. Bross[50], D. Brown[81], X.B. Bu[7], N.J. Buchanan[49], D. Buchholz[53], M. Buehler[81], V. Buescher[22], V. Bunichev[38], S. Burdin[42,b], T.H. Burnett[82], C.P. Buszello[43], J.M. Butler[62], P. Calfayan[25], S. Calvet[16], J. Cammin[71], E. Carrera[49], W. Carvalho[3], B.C.K. Casey[50], H. Castilla-Valdez[33], S. Chakrabarti[18], D. Chakraborty[52], K.M. Chan[55], A. Chandra[48], E. Cheu[45], F. Chevallier[14], D.K. Cho[62], S. Choi[32], B. Choudhary[28], L. Christofek[77], T. Christoudias[43], S. Cihangir[50], D. Claes[67], J. Clutter[58], M. Cooke[50], W.E. Cooper[50], M. Corcoran[80], F. Couderc[18], M.-C. Cousinou[15], S. Crépé-Renaudin[14], V. Cuplov[59], D. Cutts[77], M. Ćwiok[30], H. da Motta[2], A. Das[45], G. Davies[43], K. De[78], S.J. de Jong[35], E. De La Cruz-Burelo[33], C. De Oliveira Martins[3], K. DeVaughan[67], J.D. Degenhardt[64], F. Déliot[18], M. Demarteau[50], R. Demina[71], D. Denisov[50], S.P. Denisov[39], S. Desai[50], H.T. Diehl[50], M. Diesburg[50], A. Dominguez[67], H. Dong[72], T. Dorland[82], A. Dubey[28], L.V. Dudko[38], L. Duflot[16], S.R. Dugad[29], D. Duggan[49], A. Duperrin[15], J. Dyer[65], A. Dyshkant[52], M. Eads[67], D. Edmunds[65], J. Ellison[48], V.D. Elvira[50], Y. Enari[77], S. Eno[61], P. Ermolov[38,‡], H. Evans[54], A. Evdokimov[73], V.N. Evdokimov[39], A.V. Ferapontov[59], T. Ferbel[71], F. Fiedler[24], F. Filthaut[35], W. Fisher[50], H.E. Fisk[50], M. Fortner[52], H. Fox[42], S. Fu[50], S. Fuess[50], T. Gadfort[70], C.F. Galea[35], C. Garcia[71], A. Garcia-Bellido[71], V. Gavrilov[37], P. Gay[13], W. Geist[19], W. Geng[15,65], C.E. Gerber[51], Y. Gershtein[49], D. Gillberg[6], G. Ginther[71], N. Gollub[41], B. Gómez[8], A. Goussiou[82], P.D. Grannis[72], H. Greenlee[50], Z.D. Greenwood[60], E.M. Gregores[4], G. Grenier[20], Ph. Gris[13], J.-F. Grivaz[16], A. Grohsjean[25], S. Grünendahl[50], M.W. Grünewald[30], F. Guo[72], J. Guo[72], G. Gutierrez[50], P. Gutierrez[75], A. Haas[70], N.J. Hadley[61], P. Haefner[25], S. Hagopian[49], J. Haley[68], I. Hall[65], R.E. Hall[47], L. Han[7], K. Harder[44], A. Harel[71], J.M. Hauptman[57], J. Hays[43], T. Hebbeker[21], D. Hedin[52], J.G. Hegeman[34], A.P. Heinson[48], U. Heintz[62], C. Hensel[22,d], K. Herner[72], G. Hesketh[63], M.D. Hildreth[55], R. Hirosky[81], J.D. Hobbs[72], B. Hoeneisen[12], H. Hoeth[26], M. Hohlfeld[22], S. Hossain[75], P. Houben[34], Y. Hu[72], Z. Hubacek[10], V. Hynek[9], I. Iashvili[69], R. Illingworth[50], A.S. Ito[50], S. Jabeen[62], M. Jaffré[16], S. Jain[75], K. Jakobs[23], C. Jarvis[61], R. Jesik[43], K. Johns[45], C. Johnson[70], M. Johnson[50], D. Johnston[67], A. Jonckheere[50], P. Jonsson[43], A. Juste[50], E. Kajfasz[15], J.M. Kalk[60], D. Karmanov[38], P.A. Kasper[50], I. Katsanos[70], D. Kau[49], V. Kaushik[78], R. Kehoe[79], S. Kermiche[15], N. Khalatyan[50], A. Khanov[76], A. Kharchilava[69], Y.M. Kharzheev[36], D. Khatidze[70], T.J. Kim[31], M.H. Kirby[53], M. Kirsch[21], B. Klima[50], J.M. Kohli[27], J.-P. Konrath[23], A.V. Kozelov[39], J. Kraus[65], T. Kuhl[24], A. Kumar[69], A. Kupco[11], T. Kurča[20], V.A. Kuzmin[38], J. Kvita[9], F. Lacroix[13], D. Lam[55], S. Lammers[70], G. Landsberg[77], P. Lebrun[20], W.M. Lee[50], A. Leflat[38], J. Lellouch[17], J. Li[78,‡], L. Li[48], Q.Z. Li[50], S.M. Lietti[5], J.K. Lim[31], J.G.R. Lima[52], D. Lincoln[50], J. Linnemann[65], V.V. Lipaev[39], R. Lipton[50], Y. Liu[7], Z. Liu[6], A. Lobodenko[40], M. Lokajicek[11], P. Love[42], H.J. Lubatti[82], R. Luna[3], A.L. Lyon[50], A.K.A. Maciel[2], D. Mackin[80], R.J. Madaras[46], P. Mättig[26], C. Magass[21], A. Magerkurth[64], P.K. Mal[82], H.B. Malbouisson[3], S. Malik[67], V.L. Malyshev[36], Y. Maravin[59], B. Martin[14], R. McCarthy[72], A. Melnitchouk[66], L. Mendoza[8], P.G. Mercadante[5], M. Merkin[38], K.W. Merritt[50], A. Meyer[21], J. Meyer[22,d], J. Mitrevski[70], R.K. Mommsen[44], N.K. Mondal[29], R.W. Moore[6], T. Moulik[58], G.S. Muanza[20], M. Mulhearn[70], O. Mundal[22], L. Mundim[3], E. Nagy[15], M. Naimuddin[50], M. Narain[77], N.A. Naumann[35], H.A. Neal[64], J.P. Negret[8], P. Neustroev[40], H. Nilsen[23], H. Nogima[3], S.F. Novaes[5], T. Nunnemann[25], V. O'Dell[50], D.C. O'Neil[6], G. Obrant[40], C. Ochando[16], D. Onoprienko[59], N. Oshima[50], N. Osman[43], J. Osta[55], R. Otec[10], G.J. Otero y Garzón[50], M. Owen[44], P. Padley[80], M. Pangilinan[77], N. Parashar[56], S.-J. Park[22,d], S.K. Park[31], J. Parsons[70], R. Partridge[77], N. Parua[54], A. Patwa[73], G. Pawloski[80], B. Penning[23], M. Perfilov[38], K. Peters[44], Y. Peters[26], P. Pétroff[16], M. Petteni[43], R. Piegaia[1],

J. Piper[65], M.-A. Pleier[22], P.L.M. Podesta-Lerma[33,c], V.M. Podstavkov[50], Y. Pogorelov[55], M.-E. Pol[2], P. Polozov[37], B.G. Pope[65], A.V. Popov[39], C. Potter[6], W.L. Prado da Silva[3], H.B. Prosper[49], S. Protopopescu[73], J. Qian[64], A. Quadt[22,d], B. Quinn[66], A. Rakitine[42], M.S. Rangel[2], K. Ranjan[28], P.N. Ratoff[42], P. Renkel[79], P. Rich[44], J. Rieger[54], M. Rijssenbeek[72], I. Ripp-Baudot[19], F. Rizatdinova[76], S. Robinson[43], R.F. Rodrigues[3], M. Rominsky[75], C. Royon[18], P. Rubinov[50], R. Ruchti[55], G. Safronov[37], G. Sajot[14], A. Sánchez-Hernández[33], M.P. Sanders[17], B. Sanghi[50], G. Savage[50], L. Sawyer[60], T. Scanlon[43], D. Schaile[25], R.D. Schamberger[72], Y. Scheglov[40], H. Schellman[53], T. Schliephake[26], S. Schlobohm[82], C. Schwanenberger[44], A. Schwartzman[68], R. Schwienhorst[65], J. Sekaric[49], H. Severini[75], E. Shabalina[51], M. Shamim[59], V. Shary[18], A.A. Shchukin[39], R.K. Shivpuri[28], V. Siccardi[19], V. Simak[10], V. Sirotenko[50], P. Skubic[75], P. Slattery[71], D. Smirnov[55], G.R. Snow[67], J. Snow[74], S. Snyder[73], S. Söldner-Rembold[44], L. Sonnenschein[17], A. Sopczak[42], M. Sosebee[78], K. Soustruznik[9], B. Spurlock[78], J. Stark[14], J. Steele[60], V. Stolin[37], D.A. Stoyanova[39], J. Strandberg[64], S. Strandberg[41], M.A. Strang[69], E. Strauss[72], M. Strauss[75], R. Ströhmer[25], D. Strom[53], L. Stutte[50], S. Sumowidagdo[49], P. Svoisky[55], A. Sznajder[3], P. Tamburello[45], A. Tanasijczuk[1], W. Taylor[6], B. Tiller[25], F. Tissandier[13], M. Titov[18], V.V. Tokmenin[36], Y. Tschudi[20], I. Torchiani[23], D. Tsybychev[72], B. Tuchming[18], C. Tully[68], P.M. Tuts[70], R. Unalan[65], L. Uvarov[40], S. Uvarov[40], S. Uzunyan[52], B. Vachon[6], P.J. van den Berg[34], R. Van Kooten[54], W.M. van Leeuwen[34], N. Varelas[51], E.W. Varnes[45], I.A. Vasilyev[39], P. Verdier[20], L.S. Vertogradov[36], M. Verzocchi[50], D. Vilanova[18], F. Villeneuve-Seguier[43], P. Vint[43], P. Vokac[10], M. Voutilainen[67,e], R. Wagner[68], H.D. Wahl[49], M.H.L.S. Wang[50], J. Warchol[55], G. Watts[82], M. Wayne[55], G. Weber[24], M. Weber[50,f], L. Welty-Rieger[54], A. Wenger[23,g], N. Wermes[22], M. Wetstein[61], A. White[78], D. Wicke[26], M. Williams[42], G.W. Wilson[58], S.J. Wimpenny[48], M. Wobisch[60], D.R. Wood[63], T.R. Wyatt[44], Y. Xie[77], S. Yacoob[53], R. Yamada[50], W.-C. Yang[44], T. Yasuda[50], Y.A. Yatsunenko[36], H. Yin[7], K. Yip[73], H.D. Yoo[77], S.W. Youn[53], J. Yu[78], C. Zeitnitz[26], S. Zelitch[81], T. Zhao[82], B. Zhou[64], J. Zhu[72], M. Zielinski[71], D. Zieminska[54], A. Zieminski[54,‡], L. Zivkovic[70], V. Zutshi[52], and E.G. Zverev[38]

(The DØ Collaboration)

[1] *Universidad de Buenos Aires, Buenos Aires, Argentina*
[2] *LAFEX, Centro Brasileiro de Pesquisas Físicas, Rio de Janeiro, Brazil*
[3] *Universidade do Estado do Rio de Janeiro, Rio de Janeiro, Brazil*
[4] *Universidade Federal do ABC, Santo André, Brazil*
[5] *Instituto de Física Teórica, Universidade Estadual Paulista, São Paulo, Brazil*
[6] *University of Alberta, Edmonton, Alberta, Canada, Simon Fraser University, Burnaby, British Columbia, Canada, York University, Toronto, Ontario, Canada, and McGill University, Montreal, Quebec, Canada*
[7] *University of Science and Technology of China, Hefei, People's Republic of China*
[8] *Universidad de los Andes, Bogotá, Colombia*
[9] *Center for Particle Physics, Charles University, Prague, Czech Republic*
[10] *Czech Technical University, Prague, Czech Republic*
[11] *Center for Particle Physics, Institute of Physics, Academy of Sciences of the Czech Republic, Prague, Czech Republic*
[12] *Universidad San Francisco de Quito, Quito, Ecuador*
[13] *LPC, Université Blaise Pascal, CNRS/IN2P3, Clermont, France*
[14] *LPSC, Université Joseph Fourier Grenoble 1, CNRS/IN2P3, Institut National Polytechnique de Grenoble, Grenoble, France*
[15] *CPPM, Aix-Marseille Université, CNRS/IN2P3, Marseille, France*
[16] *LAL, Université Paris-Sud, IN2P3/CNRS, Orsay, France*
[17] *LPNHE, IN2P3/CNRS, Universités Paris VI and VII, Paris, France*
[18] *CEA, Irfu, SPP, Saclay, France*
[19] *IPHC, Université Louis Pasteur, CNRS/IN2P3, Strasbourg, France*
[20] *IPNL, Université Lyon 1, CNRS/IN2P3, Villeurbanne, France and Université de Lyon, Lyon, France*
[21] *III. Physikalisches Institut A, RWTH Aachen University, Aachen, Germany*
[22] *Physikalisches Institut, Universität Bonn, Bonn, Germany*
[23] *Physikalisches Institut, Universität Freiburg, Freiburg, Germany*
[24] *Institut für Physik, Universität Mainz, Mainz, Germany*
[25] *Ludwig-Maximilians-Universität München, München, Germany*
[26] *Fachbereich Physik, University of Wuppertal, Wuppertal, Germany*
[27] *Panjab University, Chandigarh, India*
[28] *Delhi University, Delhi, India*
[29] *Tata Institute of Fundamental Research, Mumbai, India*

[30] *University College Dublin, Dublin, Ireland*
[31] *Korea Detector Laboratory, Korea University, Seoul, Korea*
[32] *SungKyunKwan University, Suwon, Korea*
[33] *CINVESTAV, Mexico City, Mexico*
[34] *FOM-Institute NIKHEF and University of Amsterdam/NIKHEF, Amsterdam, The Netherlands*
[35] *Radboud University Nijmegen/NIKHEF, Nijmegen, The Netherlands*
[36] *Joint Institute for Nuclear Research, Dubna, Russia*
[37] *Institute for Theoretical and Experimental Physics, Moscow, Russia*
[38] *Moscow State University, Moscow, Russia*
[39] *Institute for High Energy Physics, Protvino, Russia*
[40] *Petersburg Nuclear Physics Institute, St. Petersburg, Russia*
[41] *Lund University, Lund, Sweden, Royal Institute of Technology and Stockholm University, Stockholm, Sweden, and Uppsala University, Uppsala, Sweden*
[42] *Lancaster University, Lancaster, United Kingdom*
[43] *Imperial College, London, United Kingdom*
[44] *University of Manchester, Manchester, United Kingdom*
[45] *University of Arizona, Tucson, Arizona 85721, USA*
[46] *Lawrence Berkeley National Laboratory and University of California, Berkeley, California 94720, USA*
[47] *California State University, Fresno, California 93740, USA*
[48] *University of California, Riverside, California 92521, USA*
[49] *Florida State University, Tallahassee, Florida 32306, USA*
[50] *Fermi National Accelerator Laboratory, Batavia, Illinois 60510, USA*
[51] *University of Illinois at Chicago, Chicago, Illinois 60607, USA*
[52] *Northern Illinois University, DeKalb, Illinois 60115, USA*
[53] *Northwestern University, Evanston, Illinois 60208, USA*
[54] *Indiana University, Bloomington, Indiana 47405, USA*
[55] *University of Notre Dame, Notre Dame, Indiana 46556, USA*
[56] *Purdue University Calumet, Hammond, Indiana 46323, USA*
[57] *Iowa State University, Ames, Iowa 50011, USA*
[58] *University of Kansas, Lawrence, Kansas 66045, USA*
[59] *Kansas State University, Manhattan, Kansas 66506, USA*
[60] *Louisiana Tech University, Ruston, Louisiana 71272, USA*
[61] *University of Maryland, College Park, Maryland 20742, USA*
[62] *Boston University, Boston, Massachusetts 02215, USA*
[63] *Northeastern University, Boston, Massachusetts 02115, USA*
[64] *University of Michigan, Ann Arbor, Michigan 48109, USA*
[65] *Michigan State University, East Lansing, Michigan 48824, USA*
[66] *University of Mississippi, University, Mississippi 38677, USA*
[67] *University of Nebraska, Lincoln, Nebraska 68588, USA*
[68] *Princeton University, Princeton, New Jersey 08544, USA*
[69] *State University of New York, Buffalo, New York 14260, USA*
[70] *Columbia University, New York, New York 10027, USA*
[71] *University of Rochester, Rochester, New York 14627, USA*
[72] *State University of New York, Stony Brook, New York 11794, USA*
[73] *Brookhaven National Laboratory, Upton, New York 11973, USA*
[74] *Langston University, Langston, Oklahoma 73050, USA*
[75] *University of Oklahoma, Norman, Oklahoma 73019, USA*
[76] *Oklahoma State University, Stillwater, Oklahoma 74078, USA*
[77] *Brown University, Providence, Rhode Island 02912, USA*
[78] *University of Texas, Arlington, Texas 76019, USA*
[79] *Southern Methodist University, Dallas, Texas 75275, USA*
[80] *Rice University, Houston, Texas 77005, USA*
[81] *University of Virginia, Charlottesville, Virginia 22901, USA and*
[82] *University of Washington, Seattle, Washington 98195, USA*

(Dated: September 2, 2008)

A search for new physics in the acoplanar jet topology has been performed in $2.5\,\mathrm{fb}^{-1}$ of data from $p\bar{p}$ collisions at $\sqrt{s}$ =1.96 TeV, recorded by the D0 detector at the Fermilab Tevatron Collider. The numbers of events with exactly two acoplanar jets and missing transverse energy are in good agreement with the standard model expectations. The result of this search has been used to set a lower mass limit of 205 GeV at the 95% C.L. on the mass of a scalar leptoquark when this particle decays exclusively into a quark and a neutrino. In the framework of the Little Higgs model with T-parity, limits have also been obtained on the T-odd quark mass as a function of the T-odd photon mass.

PACS numbers: 14.80.-j, 13.85.Rm

At hadron colliders, new colored particles predicted by various extensions of the standard model (SM) would be abundantly produced if they are light enough. The final state with jets and missing transverse energy ($\not\!\!E_T$) resulting from the decay of those particles is a promising channel to discover physics beyond the SM. In this Letter, a search for new particles in the topology consisting of exactly two jets and $\not\!\!E_T$ is presented using $2.5\,\mathrm{fb}^{-1}$ of data collected at a center-of-mass energy of 1.96 TeV with the D0 detector during Run II of the Fermilab Tevatron $p\bar{p}$ Collider. The result of this search has been used to constrain two categories of models.

The first category corresponds to models predicting the existence of leptoquarks (LQ) [1]. Those are scalar or vector particles carrying both a lepton and a baryon quantum number. They are predicted by many extensions of the SM attempting to explain the apparent symmetry between quarks and leptons. To satisfy experimental constraints on flavor changing neutral current interactions, leptoquarks couple only within a single generation. Leptoquarks decay into a charged lepton and a quark with a branching ratio β, or into a neutrino and a quark with a branching ratio $1-\beta$. Pair production of leptoquarks assuming $\beta = 0$ therefore leads only to a final state consisting of two neutrinos and two quarks. The most stringent previous limit at 95% C.L. on the scalar leptoquark mass of 136 GeV [2] for $\beta = 0$ was obtained by the D0 collaboration with $310\,\mathrm{pb}^{-1}$ of Run II data. The CDF collaboration also set a lower mass limit of 117 GeV [3] with $191\,\mathrm{pb}^{-1}$ of Run II data. Those limits, as well as the results presented in this Letter, apply for first- and second-generation scalar leptoquarks. For the third-generation, tighter limits were obtained by increasing the signal sensitivity using heavy-flavor quark tagging [4].

The second category is the Little Higgs (LH) model [5], which provides an interesting scenario for physics at the TeV scale, predicting the existence of additional gauge bosons, fermions, and scalar particles with masses in the 100 GeV – 5 TeV range. Electroweak precision constraints are satisfied by introducing a discrete symmetry called T-parity [6]. This symmetry is constructed such that all the SM states are even, while most new states of the LH model with T-parity (LHT) are odd. In the LHT model, six new Dirac T-odd quarks (T-quarks or $\tilde{Q}$) are the partners of the left handed T-even quarks of the SM. In most of the parameter space, the lightest T-odd particle (LTP) is the so-called "heavy photon" ($\tilde{A}_H$) which is stable and weakly interacting. From SM precision measurements, it is possible to set a lower mass limit of ∼80 GeV on the mass of $\tilde{A}_H$ [7]. The new particle spectrum of the LHT model has similar properties to spectra of supersymmetric models. The LTP, just as the Lightest Supersymmetric Particle in SUSY models with R-parity conservation, is a dark matter candidate which escapes undetected. There are, however, important differences: the new T-odd particles have the same spin as their SM partner; and in the LHT model, some SM states, for example right-handed SM fermions or gluons, have no partners. In the following, the mass of the T-quarks from the first two generations is assumed to be degenerate, and pair production of those four T-quarks is considered. As the T-odd gauge bosons other than the $\tilde{A}_H$ are relatively heavy, T-quarks decay into a quark and $\tilde{A}_H$ in most of the parameter space accessible at the Tevatron. It will be assumed in the following that this branching ratio is 100%. Pair production of T-quarks therefore leads to a final state with two quarks and two LTP, giving the missing transverse energy signature. The only direct constraint from collider data on the T-quark mass is the ∼100 GeV lower limit on the mass of the supersymmetric partner of the first two generations quarks from LEP [8] which can also be applied to T-quarks. Prospective studies [9] have shown that the Tevatron can be sensitive to T-quark masses up to ∼400 GeV. This sensitivity is severely reduced when the mass difference between the T-quarks and the LTP becomes small.

The D0 detector has been described in detail in Ref. [10]. Tracks are reconstructed in a silicon microstrip tracker and a central fiber tracker (CFT), both located within a 2 T superconducting solenoidal magnet. The liquid argon and uranium calorimeter consists of three cryostats. The central one covers pseudorapidities [11] $|\eta| \lesssim 1.1$, and the two end sections extend the coverage up to $|\eta| \approx 4.2$. The calorimeter is designed in projective towers of size 0.1×0.1 in the (η, ϕ) plane, where ϕ is the azimuthal angle in radians. The outer muon system, covering $|\eta| < 2$, consists of tracking detectors and scintillation trigger counters in front of 1.8 T iron toroids, followed by two similar layers after the toroids.

Jets were reconstructed with the iterative midpoint cone algorithm [12] with cone radius $\mathcal{R} = \sqrt{(\Delta\phi)^2 + (\Delta y)^2} = 0.5$ in azimuthal angle ϕ and rapidity $y = \frac{1}{2}\ln[(E+p_z)/(E-p_z)]$. The jet energy scale (JES) corrections were derived from the transverse momentum balance in photon-plus-jet events. The $\not\!\!E_T$ was calculated from all calorimeter cells, and corrected for the jet energy scale and for the transverse momenta of reconstructed muons.

In events from SM processes, the presence of neutrinos from W or Z decay in the final state generates large $\not\!\!E_T$. The main irreducible SM background in this search for new particles is therefore the $Z(\to \nu\bar{\nu})$+jets process. The $W(\to l\nu)$+jets events also exhibit the $\not\!\!E_T$ signature, but their contribution can be significantly reduced by rejecting events with an isolated electron or muon. How-

ever, the charged lepton can escape detection in uninstrumented regions of the detector, fail identification criteria, or be a tau lepton decaying hadronically. To further suppress that background, events containing an isolated high p_T track are rejected. The other SM backgrounds for this search are the pair production of vector bosons (WW, WZ, ZZ) and the production of top quarks, either in pairs ($t\bar{t}$) or via the electroweak interaction. Finally, multijet production when one or more jets are mismeasured also leads to a final state with jets and $\not\!\!E_T$ ("QCD background").

Events from SM processes and signal events were simulated using Monte Carlo (MC) generators and passed through a full GEANT3-based [13] simulation of the detector geometry and response. They were subsequently processed with the same reconstruction chain as the data. The parton distribution functions (PDFs) used in the MC generators are the CTEQ6L1 [14] PDFs. A data event from a randomly selected beam crossing was overlaid on each event to simulate the additional minimum bias interactions and detector noise. The ALPGEN generator [15] was used to simulate $W/Z+$jets and $t\bar{t}$ production. It was interfaced with PYTHIA [16] for the simulation of initial and final state radiation (ISR/FSR) and of jet hadronization. Pairs of vector bosons and electroweak top quark production were simulated with PYTHIA and COMPHEP [17], respectively. The next-to-leading order (NLO) cross sections were computed with MCFM 5.1 [18]. The QCD background was not simulated, since it can be conservatively neglected in the final stage of this analysis.

Leptoquark pair production and decays were simulated with PYTHIA and the CTEQ6L1 PDFs. The LQ mass in the MC simulation ranged from 60 to 240 GeV. The NLO cross sections of this process were computed from a program based on [19] with a renormalization and factorization scale ($\mu_{\rm r,f}$) equal to the LQ mass, and using the CTEQ6.1M PDF sets.

For the LHT model, it has been shown in [9] that T-quark pair production and decay to $q\tilde{A}_H$ is very similar to squark pair production and decay to $q\tilde{\chi}_1^0$, where $\tilde{\chi}_1^0$ is the lightest neutralino. Signal efficiencies were therefore determined using MC events generated with PYTHIA corresponding to the production and decay of these supersymmetric particles. It has been checked that the spin differences between the T-odd particles of the LHT model and the supersymmetric particles do not modify the signal efficiencies. Therefore, MC simulations of such events were performed to cover the $\tilde{Q}$–$\tilde{A}_H$ mass plane accessible at the Tevatron. Concerning the signal normalization, the cross section of first and second generation T-quark pair production is equal to four times the cross section of heavy quark pair production, if no other new particles predicted by the LHT model are involved in the T-quark production. The NLO cross sections of this signal were therefore calculated using MCFM 5.1, with $\mu_{\rm r,f}$ equal to the T-quark mass, and the CTEQ6.1M PDF sets.

The analysis strategy follows closely the "dijet" analysis from Ref. [20]. Events were recorded using triggers requiring two acoplanar jets and large $\not\!\!E_T$ or $\not\!\!H_T$, where $\not\!\!H_T$ is the vector sum of the jet transverse momenta ($\not\!\!H_T = |\sum_{\rm jets} \overrightarrow{p_T}|$). The trigger requirements evolved during the Run II data taking period in order to take into account the increasing peak instantaneous luminosity of the Tevatron. At the last stage of the trigger selection, the requirements were typically the following: (1) $\not\!\!E_T$ or $\not\!\!H_T$ greater than 30 GeV and their separation from all jets greater than 25°; (2) an azimuthal angle between the two highest p_T jets less than 170°. Offline, events where $\not\!\!E_T$ was higher than 40 GeV were then selected. The best primary vertex (PV0) was defined as the vertex with the smallest probability to be due to a minimum bias interaction [21]. The longitudinal position of PV0 was required to be less than 60 cm from the detector center to ensure efficient vertex reconstruction. Good jets were defined as jets with a fraction of energy in the electromagnetic layers of the calorimeter lower than 0.95. The acoplanarity, i.e. the azimuthal angle between the two leading jets, $\rm jet_1$ and $\rm jet_2$, ordered by decreasing transverse momentum, was required to be less than 165 degrees. Then, the two leading jets were required to be in the central region of the detector, with $|\eta_{\rm det}| < 0.8$, where $\eta_{\rm det}$ is the jet pseudorapidity calculated under the assumption that the jet originates from the detector center. After this preselection, the transverse momenta of the two leading jets had to be higher than 35 GeV. Finally, jets were required to originate from the best primary vertex, based on their associated tracks [20]. This was accomplished by requiring CPF0 > 0.75, where CPF0 is the fraction of track p_T sum associated with the jet which comes from PV0, CPF0$= \sum p_T^{\rm track}({\rm PV0}) / \sum p_T^{\rm track}({\rm any\ PV})$.

At this stage, the QCD multijet background is still largely dominant. To further reject those events, the selection criteria on $\not\!\!E_T$ was increased to 75 GeV. The requirement that the azimuthal angle between the $\not\!\!E_T$ and the first jet, $\Delta\phi(\not\!\!E_T, {\rm jet_1})$, exceeds 90 degrees, was used to remove events where a jet was mismeasured and generating $\not\!\!E_T$ aligned to that jet. Also, the minimal azimuthal angle $\Delta\phi_{\rm min}(\not\!\!E_T, {\rm any\ jet})$ and the maximal azimuthal angle $\Delta\phi_{\rm max}(\not\!\!E_T, {\rm any\ jet})$ between jets and $\not\!\!E_T$ directions had to be greater than 50 degrees and lower than 170 degrees, respectively.

To suppress $W(\to l\nu)+$jets events, a veto on events containing an isolated electron or muon with $p_T > 10$ GeV was applied. Events with an isolated track were then rejected to further reduce that background. Isolated tracks were required to have $p_T > 5$ GeV, to originate from PV0 with $DCA(z) < 5$ cm and $DCA(r) < 2$ cm, where $DCA(z)$ and $DCA(r)$ are the positions of the projection of the distance of closest approach between the track and PV0 on the beam direction and in the plane transverse to the beamline, respectively. The number of hits in the CFT used to

TABLE I: Number of events observed, expected from background and signal MC simulations, and signal efficiencies for $M_{LQ} = 200\,\text{GeV}$ at the various stages of the analysis. The QCD multijet contribution is not included in the background contribution. The quoted uncertainties are the combined statistical and systematic uncertainties.

Cut applied	Data	Background	Signal	Signal efficiency
Preselection	208,055	$30,752 \pm 5350$	166 ± 21	0.302 ± 0.037
1st leading jet $p_T > 35\,\text{GeV}$[a]	122,456	$25,352 \pm 4410$	152 ± 19	0.276 ± 0.034
2nd leading jet $p_T > 35\,\text{GeV}$[a]	79,985	$14,538 \pm 2530$	144 ± 18	0.262 ± 0.032
$\not\!\!E_T > 75$ GeV	6,509	$5,219 \pm 909$	125 ± 16	0.228 ± 0.028
$\Delta\phi(\not\!\!E_T, \text{jet}_1) > 90^\circ$	6,386	$5,148 \pm 897$	124 ± 15	0.226 ± 0.028
$\Delta\phi_{\min}(\not\!\!E_T, \text{any jet}) > 50^\circ$	3,857	$3,453 \pm 602$	93 ± 12	0.170 ± 0.021
$\Delta\phi_{\max}(\not\!\!E_T, \text{any jet}) < 170^\circ$	2,855	$2,568 \pm 448$	81 ± 10	0.147 ± 0.018
Isolated electron veto	2,347	$2,129 \pm 371$	79.1 ± 9.8	0.144 ± 0.018
Isolated muon veto	2,007	$1,880 \pm 328$	79.1 ± 9.8	0.144 ± 0.018
Isolated track veto	1,472	$1,398 \pm 244$	73.0 ± 9.1	0.133 ± 0.017
Exactly two jets	957	858 ± 150	49.1 ± 6.1	0.089 ± 0.011
Final H_T cut			optimized	
Final $\not\!\!E_T$ cut			optimized	

[a]First and second jets are also required to be central ($|\eta_{\text{det}}| < 0.8$), with an electromagnetic fraction below 0.95, and to have CPF0 ≥ 0.75.

reconstruct the track was required to be at least 8. Finally, good quality tracks were selected by requiring the χ^2/dof of the track-fit reconstruction to be lower than 4. A hollow cone with inner and outer radii of 0.06 and 0.5 was constructed around each track that passed those criteria. If no other track with $p_T > 0.5\,\text{GeV}$ and the same quality criteria as above was found in this hollow cone, the track was considered isolated. The use of a hollow, rather than full cone also allowed rejection of tau leptons decaying into three charged particles.

Events with exactly two jets with $p_T > 15\,\text{GeV}$ and $|\eta_{det}| < 2.5$ in the final state were then selected. This criterion rejects a large fraction of the remaining $t\bar{t}$ events, and increases the signal sensitivity at large T-quark and leptoquark masses once large $\not\!\!E_T$ and H_T are required, with $H_T = \sum_{\text{jets}} p_T$, where the sum is also over all jets with $p_T > 15\,\text{GeV}$ and $|\eta_{\text{det}}| < 2.5$. Table I summarizes the number of events observed and expected from MC simulations at each stage of the analysis. Figure 1 shows comparisons between data and MC simulations: the distribution of the number of jets, and the $\not\!\!E_T$ and H_T distributions after applying all the selection criteria described above.

Finally, the two final cuts on $\not\!\!E_T$ and on H_T were optimized for different signals by minimizing the expected upper limit on the cross section in the absence of signal. To this end and also for the final limit computation, the CLs modified frequentist method has been used [22]. For the leptoquark search, two benchmarks were defined corresponding to low ($M_{LQ} = 140\,\text{GeV}$) and high ($M_{LQ} = 200\,\text{GeV}$) leptoquark masses. As summarized in Table II, the optimized values were determined to be $H_T > 150\,\text{GeV}$ and $\not\!\!E_T > 75\,\text{GeV}$ for the low mass selection, and $H_T > 300\,\text{GeV}$ and $\not\!\!E_T > 125\,\text{GeV}$ for the high mass selection. In the T-quark search, five H_T–$\not\!\!E_T$ cut combinations were used to optimally scan the $(\tilde{Q}, \tilde{A}_H)$ mass plane as summarized in Table II. In all cases, the contribution of the QCD multijet background was estimated to be small enough to be conservatively neglected. The number of events observed are in good agreement with the SM expectations.

The uncertainty coming from the JES corrections on the SM backgrounds and signal predictions ranges from 5% for low H_T and $\not\!\!E_T$ cuts to 10% for high H_T and $\not\!\!E_T$ cuts. The uncertainties due to the jet energy resolution, to the jet track confirmation, and to jet reconstruction and identification efficiencies range between 2% and 4%. The systematic uncertainty due to the isolated track veto was measured to be 3%. All these uncertainties account for differences between data and MC simulation, both for signal efficiencies and background contributions. The trigger was found to be fully efficient for the event samples surviving all analysis requirements within an uncertainty of 2%. The uncertainty on the luminosity measurement is 6.1% [23]. All of these uncertainties are fully correlated between signal and SM backgrounds. A 15% systematic uncertainty was set on the W/Z+jets and $t\bar{t}$ NLO cross sections. The uncertainty on the signal acceptance due to the PDF choice was determined to be 6%, using the forty-eigenvector basis of the CTEQ6.1M PDF set [14]. Finally, the effects of ISR/FSR on the signal efficiencies were studied by varying the PYTHIA parameters controlling the QCD scales and the maximal allowed virtualities used in the simulation of the space-like and time-like parton showers. The uncertainty on the signal efficiencies was determined to be 6%.

The nominal NLO signal cross sections, σ_{nom}, were computed with the CTEQ6.1M PDF and for the renormalization and factorization scale $\mu_{\text{r,f}} = Q$, where Q was taken to be equal to the leptoquark or T-quark mass.

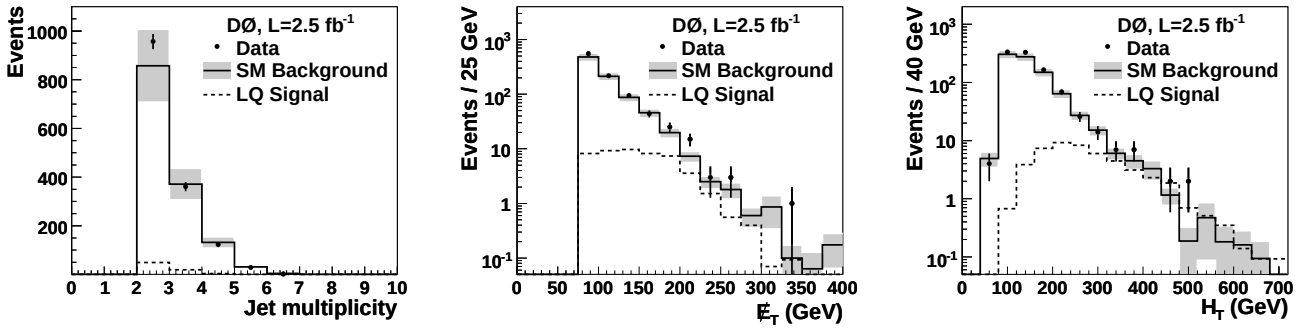

(a) (b) (c)

FIG. 1: Distribution of the number of jets (a) and distributions of $\not\!\!E_T$ (b) and H_T (c) before the final optimization of the cuts on these two quantities; for data (points with error bars), for SM background (full histogram with shaded band corresponding to the total uncertainty), and for signal MC (dashed histogram). The signal drawn corresponds to pair production of scalar leptoquarks with $M_{LQ} = 200\,\text{GeV}$.

TABLE II: For each optimized event selection, information on the signal for which it was optimized (M_{LQ} or $(M_{\tilde{Q}}, M_{\tilde{A}_H})$, and nominal NLO cross section), lower values of H_T and $\not\!\!E_T$ selection criteria, the number of events observed, the number of events expected from SM backgrounds, the number of events expected from signal, and the 95% C.L. signal cross section upper limit. The first uncertainty is statistical and the second one is systematic.

M_{LQ} or $(M_{\tilde{Q}}, M_{\tilde{A}_H})$ (GeV)	σ_{nom} (pb)	$(H_T, \not\!\!E_T)$ (GeV)	N_{obs}	$N_{\text{backgrd.}}$	$N_{\text{sig.}}$	σ_{95} (pb)
Leptoquark search						
140	2.38	(150, 75)	353	$328 \pm 11^{+56}_{-57}$	$229 \pm 8^{+24}_{-23}$	1.79
200	0.268	(300, 125)	12	$10.6 \pm 1.7^{+4.0}_{-2.0}$	$13.7 \pm 0.6^{+1.8}_{-2.0}$	0.240
T-quark search						
(150,100)	59.6	(125, 75)	566	$513 \pm 14^{+86}_{-87}$	$879 \pm 167^{+108}_{-94}$	17.0
(250,175)	3.18	(175, 100)	147	$140 \pm 7^{+25}_{-26}$	$83 \pm 12^{+16}_{-10}$	2.42
(300,200)	0.868	(225, 125)	44	$40 \pm 4^{+7}_{-7}$	$25.7 \pm 3.4^{+4.3}_{-4.7}$	0.780
(350,200)	0.242	(275, 150)	15	$13.1 \pm 2.1^{+2.6}_{-2.7}$	$16.4 \pm 1.5^{+3.1}_{-3.0}$	0.169
(400,150)	0.0666	(325, 175)	7	$4.2 \pm 1.0^{+1.2}_{-0.9}$	$10.1 \pm 0.6^{+1.2}_{-1.5}$	0.0593

The uncertainty due to the choice of PDF was determined using the full set of CTEQ6.1M eigenvectors, with the individual uncertainties added in quadrature. The effect of the renormalization and factorization scale was studied by calculating the signal cross sections for $\mu_{\text{r,f}} = Q$, $\mu_{\text{r,f}} = Q/2$ and $\mu_{\text{r,f}} = 2 \times Q$. The PDF and $\mu_{\text{r,f}}$ effects were added in quadrature to compute minimum, σ_{min}, and maximum, σ_{max}, signal cross sections.

For the leptoquark search, Fig. 2 shows the 95% C.L. observed and expected upper limits on scalar leptoquark production cross sections. The intersection with the minimal NLO cross section gives a lower mass limit of 205 GeV for $\beta = 0$. The corresponding expected limit is 207 GeV. Those limits are 214 GeV and 222 GeV, respectively, for the nominal signal cross section.

For the T-quark search, Fig. 3 shows the 95% C.L. excluded regions in $\tilde{Q}$–$\tilde{A}_H$ mass plane assuming that the branching fraction of the decay $\tilde{Q} \to q\tilde{A}_H$ is 100%. The largest excluded T-quarks mass, 404 GeV, is obtained for large mass difference between the T-quarks and the LTP.

In summary, a search for scalar leptoquarks and for T-quarks produced in $p\bar{p}$ collisions at $\sqrt{s}$ =1.96 TeV has been performed with a 2.5 fb^{-1} data sample. This search was conducted in events containing exclusively two jets and large missing transverse energy. The results are in good agreement with the SM background expectations, and 95% C.L. limits have been set on the leptoquark and T-quark masses. For a single-generation scalar leptoquark, a lower mass limit of 205 GeV has been obtained for $\beta = 0$, improving the previous limit by 69 GeV. In the LHT model, limits on T-quark mass were obtained as a function of the $\tilde{A}_H$ mass assuming 100% branching ratio for the decay $\tilde{Q} \to q\tilde{A}_H$. T-quark masses up to 404 GeV are excluded when the mass difference between T-quarks and the LTP is large. Those are the most stringent direct limits to date on the T-quarks mass.

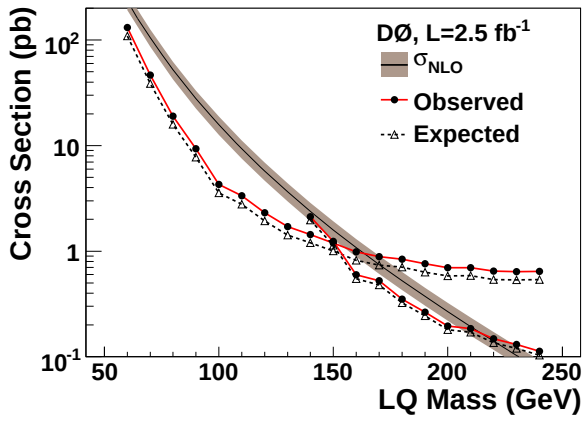

FIG. 2: For the leptoquark search, observed (circles) and expected (triangles) 95% C.L. upper limits on scalar leptoquark production cross sections. The limits obtained with the low mass and high mass selections are shown separately. The nominal production cross sections are also shown for $\beta = 0$, with shaded bands corresponding to the PDF and renormalization and factorization scale uncertainties.

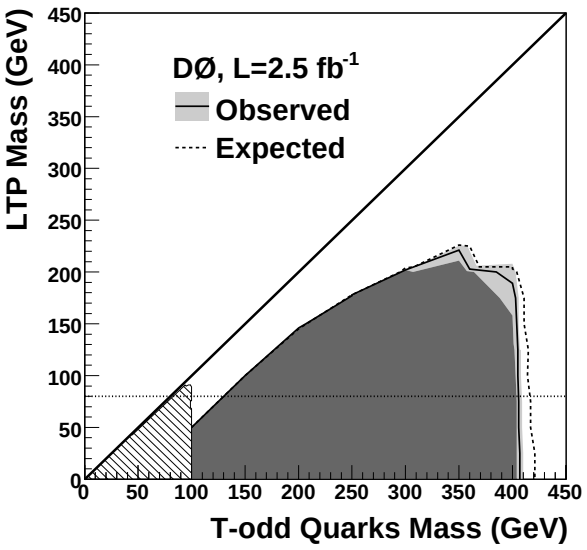

FIG. 3: For the T-quark search, expected and observed 95% C.L. excluded regions in the $\tilde{Q}$–$\tilde{A}_H$ mass plane. The dark shaded region is the observed exclusion for the minimal signal cross section hypothesis. The light shaded band shows the effect on the observed exclusion coming from the theoretical uncertainty on the signal cross section. The full and dotted black lines are the observed and expected limits, respectively, for the nominal cross section hypothesis. The hatched region is excluded by LEP [8]. The region below the horizontal dashed line ($M_{\tilde{A}_H} < 80\,\text{GeV}$) is excluded by SM precision measurements [7].

We thank M. Carena, J. Hubisz, and M. Perelstein for their valuable help with the LHT model, the staffs at Fermilab and collaborating institutions, and acknowledge support from the DOE and NSF (USA); CEA and CNRS/IN2P3 (France); FASI, Rosatom and RFBR (Russia); CNPq, FAPERJ, FAPESP and FUNDUNESP (Brazil); DAE and DST (India); Colciencias (Colombia); CONACyT (Mexico); KRF and KOSEF (Korea); CONICET and UBACyT (Argentina); FOM (The Netherlands); STFC (United Kingdom); MSMT and GACR (Czech Republic); CRC Program, CFI, NSERC and WestGrid Project (Canada); BMBF and DFG (Germany); SFI (Ireland); The Swedish Research Council (Sweden); CAS and CNSF (China); and the Alexander von Humboldt Foundation (Germany).

[a] Visitor from Augustana College, Sioux Falls, SD, USA.
[b] Visitor from The University of Liverpool, Liverpool, UK.
[c] Visitor from ECFM, Universidad Autonoma de Sinaloa, Culiacán, Mexico.
[d] Visitor from II. Physikalisches Institut, Georg-August-University, Göttingen, Germany.
[e] Visitor from Helsinki Institute of Physics, Helsinki, Finland.
[f] Visitor from Universität Bern, Bern, Switzerland.
[g] Visitor from Universität Zürich, Zürich, Switzerland.
[‡] Deceased.

[1] J.C. Pati and A. Salam, Phys. Rev. D **10**, 275 (1974); H. Georgi and S. Glashow, Phys. Rev. Lett. **32**, 438 (1974); B. Schrempp and F. Schrempp, Phys. Lett. B**153**, 101 (1985).
[2] V.M. Abazov *et al.* [DØ Collaboration], Phys. Lett. B**640**, 230 (2006).
[3] D.E. Acosta *et al.* [CDF Collaboration], Phys. Rev. D **71**, 112001 (2005) [Erratum-ibid. D **71**, 119901 (2005)].
[4] V.M. Abazov *et al.* [DØ Collaboration], Phys. Rev. Lett. **99**, 061801 (2007).
[5] N. Arkani-Hamed, A.G. Cohen, E. Katz and A.E. Nelson, JHEP **0207**, 034 (2002).
[6] H.C. Cheng and I. Low, JHEP **0309**, 051 (2003); JHEP **0408**, 061 (2004).
[7] J. Hubisz, P. Meade, A. Noble and M. Perelstein, JHEP **0601**, 135 (2006).
[8] A. Heister et al. (ALEPH Collaboration), Phys. Lett. B**537**, 5 (2002); P. Achard et al. (L3 Collaboration), Phys. Lett. B**580**, 37 (2004).
[9] M.S. Carena, J. Hubisz, M. Perelstein and P. Verdier, Phys. Rev. D **75**, 091701 (2007).
[10] V.M. Abazov *et al.* (D0 Collaboration), Nucl. Instrum. Methods in Phys. Res. A **565**, 463 (2006).
[11] The pseudorapidity η is defined as $-\ln[\tan(\theta/2)]$, with θ being the polar angle with respect to the proton beam direction.
[12] G.C. Blazey *et al.*, arXiv:hep-ex/0005012 (2000).
[13] R. Brun and F. Carminati, CERN Program Library Long Writeup W5013, 1993 (unpublished).
[14] J. Pumplin *et al.*, JHEP **0207**, 012 (2002); D. Stump *et al.*, JHEP **0310**, 046 (2003).

[15] M.L. Mangano *et al.*, JHEP **0307**, 001 (2003); versions 2.05 and 2.11 were used.
[16] T. Sjöstrand, S. Mrenna and P. Skands, JHEP **0605**, 026 (2006); versions 6.323 and 6.409 were used.
[17] E. Boos *et al.* (CompHEP Collaboration), Nucl. Instrum. Methods in Phys. Res. A **534**, 250 (2004).
[18] J.M. Campbell and R.K. Ellis, Phys. Rev. D **60**, 113006 (1999).
[19] M. Kramer *et al.*, Phys. Rev. Lett. **79**, 341 (1997).
[20] V.M. Abazov *et al.* (D0 Collaboration), Phys. Lett. B**660**, 449 (2008).
[21] V.M. Abazov *et al.* (D0 Collaboration), Phys. Rev. D **74**, 112004 (2006).
[22] T. Junk, Nucl. Instrum. Methods in Phys. Res. A **434**, 435 (1999); A. Read, in *"1st Workshop on Confidence Limits,"* CERN Report No. CERN-2000-005, 2000; W. Fisher, FERMILAB-TM-2386-E (2007).
[23] T. Andeen *et al.*, FERMILAB-TM-2365 (2007).